

CORROSION OF A CARBON STEEL COVERED BY TREATED BENTONITES IN AQUEOUS SOLUTION

F. Arbaoui^{*1}, S. A. Amzert¹, M. N. Boucherit²

¹Centre de Recherche Nucléaire de Birine, BP 180, Ain Oussera, W. Djelfa 17200, Algérie.

²Unité de Recherche et Développement de l'Ingénierie Nucléaire, Commissariat à l'Energie Atomique, BP 399 Alger, Algérie

Received: 12 January 2017 / Accepted: 22 July 2017 / Published online: 01 September 2017

ABSTRACT

In the present work we realised an electrochemical system for steel/clay/aqueous solutions study. Two Algerian bentonites have been considered. The obtained results show that both clays are corrosive even in the absence of chloride ions. We show that this corrosiveness is related to the cationic exchange capacity (CEC). The chemical treatment of clays by tungstate reduces significantly their CEC and corrosiveness. Electrochemical impedance spectroscopy results prove that tungstate reduces iron and chlorides ions transport through the clay. This deduction is supported also by microscopic observations.

Keywords: Corrosion inhibitor, Carbon steel, Electrochemical Impedances Spectroscopy; Algerian bentonites; Tungstate.

Author Correspondence, e-mail: arfahd2@yahoo.fr

doi: <http://dx.doi.org/10.4314/jfas.v9i3.4>

1. INTRODUCTION

Radioactive waste storage studies have been initiated for some decades [1]. If multiple issues were considered, few countries, especially those involved in nuclear waste production, were seriously interested by the subject. Various concepts have been developed for High Level Nuclear Waste disposal [2-4]. The multi barrier system was however the most studied and usually adopted. In this system, the waste is vitrified and stored in metal containers. The containers are wrapped by a swelling material such as bentonite and stored in deep geological



sites. The aim is to put sensitive materials out of reach while allowing their recovering for an eventual recycle as fuel for advanced technologies [5]. A valuable review of underground repositories experiences has been made by Remppe [6] where he concludes that geological isolation of radioactive waste is safe and can be considered as a permanent solution. Long-term modelling studies confirm also the robustness of this technological option [7]. However, the integrity of the system depends considerably on the corrosion resistance of the containers [8, 9].

The corrosion of materials in clay environment is different from that in aqueous solution. This is mainly due to the impermeability of the clay but also to the absence of hydroxide ions and diffusion/migration of dissolved metallic ions [10]. Quantified measures confirmed that the layer of corrosion products formed on the steel surface remains thinner than in aqueous solutions [11]. More precisely, it has been found that the corrosion process is affected at its first stage by the clay [12]; The montmorillonite contained in the clay interacts with the metal and blocks partially the surface reducing general corrosion and supporting localized corrosion.

From an opposite point of view, the alteration of the clay by corrosion products has also been studied. Bildstein underlines the fact that corrosion products interact with the clay by ion exchange causing the alteration of its properties [13]. These alterations are supposed to affect mainly the structure of the clay [11, 14].

Although generic factors can occur in the corrosion of a material in a clay, the corrosion performance of a material irrefutably depends on the specific characteristics of the surrounding clay.

In this study, we are interested by the corrosiveness of two Algerian clays and their ability to absorb tungstate which is known to be a good corrosion inhibitor in aqueous solutions [15-19]. The difference between the two clays and the efficiency of tungstate are discussed on the basis of the cation exchange capacity.

2. MATERIALS AND METHODS

All electrochemical experiments were conducted on a three phase system: carbon steel/clay/aqueous solution. The chemical composition of the carbon steel are (wt%) C 0.18, Si 0.22, Mn 0.52, Ni 0.04, Ti 0.01, P 0.01, Cu 0.63, Mo 0.02 and Fe balance. Before the experiment, the steel is covered by the studied clay which has been initially damped by the

solution: Fig. 1. The electrode is maintained horizontally in order to ensure the firmness of the clay.

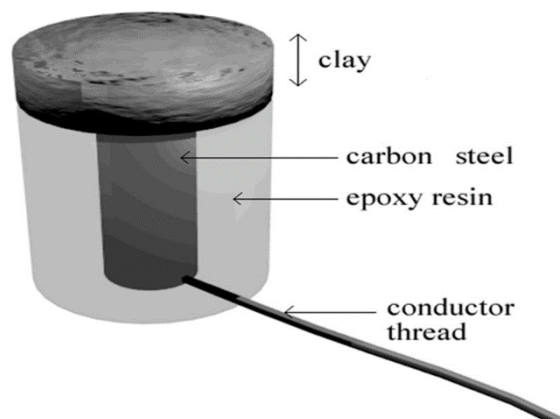


Fig.1. Working electrode made of carbon steel covered by bentonite.

Two different clays have been studied. The clay designated by Mos come from the deposit of M'Zila in Mostaganem region. While Mag come from the deposit of Hammam Boughrara in Maghnia region. The phase composition of both materials is shown in Table 1 [17].

Table 1. Phase composition of the two studied bentonites.

Bentonites	Mag (wt%)	Mos (wt%)
Phases		
Montmorillonite	65-70	45-50
Illite	1-2	8-10
Illite/Smectite	minor	minor
Quartz	15-20	15-20
Calcite	1-2	2
Feldspaths K	5-10	3-5

In most cases the clays were treated in order to insert specific cations: Na^+ , K^+ or Ca^{2+} . To do this insertion we put 50 g of raw bentonite into 1 litre of normal chloride solution: NaCl, KCl or CaCl_2 . The suspension is shaken for 6 hours and then decanted. The supernatant is then removed and the operation is repeated three times. The salt excess is eliminated by washing the sample repeatedly with deionised water. At the end the chemically treated bentonite is dried and grinded. In the text, for example, Mos-Na means the Mos bentonite treated by NaCl.

In some experiments we incorporated tungstate anions into the clay. In this work tungstate is considered as a corrosion inhibitor. To incorporate WO_4^{2-} we put 50 g of the bentonite in 1 litre of Na_2WO_4 0.5M solution. The suspension is shaken for 6 hours and then decanted. The supernatant is removed and the operation is repeated three times. The enriched bentonite is then dried and grinded. In the text the notation Mos-W means the Mos bentonite enriched by Na_2WO_4 . The tungstate proportion after the incorporation operation has been determined by Neutron Activation Analysis. Results are reported in Table 2. A dedicated paper explaining the technique has been published [20].

Table 2. Tungsten ratio and CEC value for Mag-Na and Mos-Na before and after tungstate treatment

	Wt %	CEC meq g/100g
Mag-Na	6.60 10^{-4}	109.41
Mag-Na treated with tungstate	25.99	90.66
Mos-Na	0.90 10^{-4}	62.52
Mos-Na treated with tungstate	19.99	29.69

The reactivity of clay depends closely on its ability to exchange cations. The cationic exchange capacity CEC describes how many mg of cations are exchanged by 100 g of the clay. In this work we used the spot test procedure for determining the CEC. A detailed description of this procedure can be found in the reference [21].

The electrochemical measures were conducted using a PARSTAT 2273 potentiostat. All voltammograms have been obtained by potential sweeping at 1mV/s between -1100 mV/SCE and +1000 mV/SCE. The electrochemical impedance spectroscopy (EIS) tests were performed around the OCP with amplitude current of ± 10 mV. The frequencies for EIS tests were set from 100 kHz to 10 mHz, and analysed using a ZSimpWin software. The surface observations have been obtained with a Microscope Leica M320.

3. RESULTS AND DISCUSSION

Steel/water systems are relatively simple configurations in corrosion studies; but investigations turn to be more complicated with the presence of intermediate clay. This complexity is due to the increased number of phases and interfaces; as well as the composition and heterogeneity of clay. So thickness and chemical pre-treatments of the clay must influence the corrosion process.

Fig. 2 illustrates the influence of a clay layer on the electrochemical reactions of steel in an aerated solution. The figure gathers three voltammogram curves obtained with a carbon steel surface: (a) exposed to an aerated 0.01M NaCl solution; (b) exposed to a de-aerated 0.01M NaCl solution, (c) covered by Mag-Na and exposed to an aerated 0.01M NaCl solution. In the first case, the corrosion potential E_{corr} appears at -400 mV/SCE. In the second case, where no oxygen is available, a substantial cathodic shift of the corrosion potential is noted. In the third case, which corresponds to the steel/clay/water system, a cathodic displacement of E_{corr} is also observed. As the corrosion potential is fixed by all anodic and cathodic reactions occurring at the electrode surface the cathodic displacement of E_{corr} must be related to the decrease of the cathodic current and therefore to the lack of oxygen to be reduced. Thus, the presence of the clay must prevent oxygen diffusion to the steel surface regardless of the aeration of the solution [12].

In the steel/solution systems we can see that the shapes of curves (a) and (b) are quite similar. A current shoulder can be seen above the corrosion potential. This phenomenon could be related to the dissolution precipitation mechanism occurring during passive film formation [22, 23]. But with the steel/clay/solution system there is no current shoulder and the anodic current density is even more important. In this case, Fe^{2+} oxidised species cannot react with hydroxide ions to form a passive film. By increasing the potential, iron dissolution continues and must depend only on the clay properties.

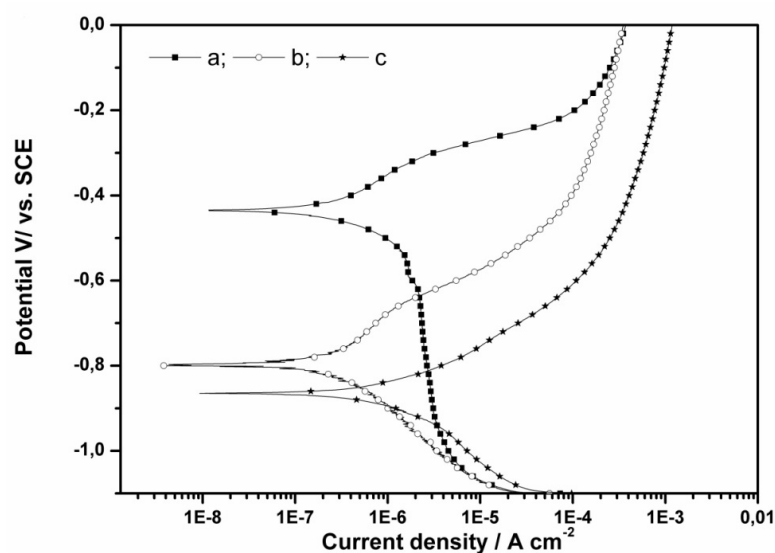


Fig.2. Potentiodynamic curves of carbon steel exposed to 0.01M NaCl solution (a) aerated solution, (b) de-aerated solution by N_2 bubbling (c) aerated solution and surface covered by Mag-Na bentonite.

Now the question is: How important is this iron dissolution when the thickness of the clay increases and after a specific pre-treatment.

In Table 3 open circuit potentials are gathered. They are obtained with iron/Mag-Na/NaCl system. Each row corresponds to a specific pre-treatment carried out on the clay. Results show that E_{corr} depends only on the presence or the absence of the clay. A long or short pre-treatment with or without NaCl does not affect E_{corr} . For this reason and for all the remaining experiences, the thickness of the clay deposit is fixed to 0.50 mm.

Table 3. Variation of the open circuit potential in mV/SCE in function of the thickness of the clay and its pretreatment

Clay thickness [mm]	0.50	1	2	5
Wetting by deionised water	-842.60	-867.10	-864.20	-859.30
Wetting by NaCl solution	-865.50	-874.60	-871.70	-869.40
Wetting by deionised water during 36 hours	-852.40	-873.50	-875.70	-865.50
Wetting by NaCl solution during 36 hours	-852.20	-879.30	-843.30	-848.30

Beyond the thickness and pre-treatments, the bulk composition of the clay must also influence the reactions at the steel/clay interface. In this study, we were interested by the comparison of two local bentonites. Fig. 3 gathers voltammograms obtained in chloride solutions with carbon steel surface covered by Mos-Na (b) and Mag-Na (c). A third curve (a) was obtained without clay deposit. By comparing these curves we can underline two main observations: steel/clay/solution systems present an important anodic current density. The slope of the current density curve is more important with Mag-Na than Mos-Na. Clay aggressiveness has been in fact reported by some authors [10, 24]. It must be due to the dissolution without precipitation of iron in the clay. In addition, the difference in corrosiveness between the two clays must be related to their different cationic exchange capacity.

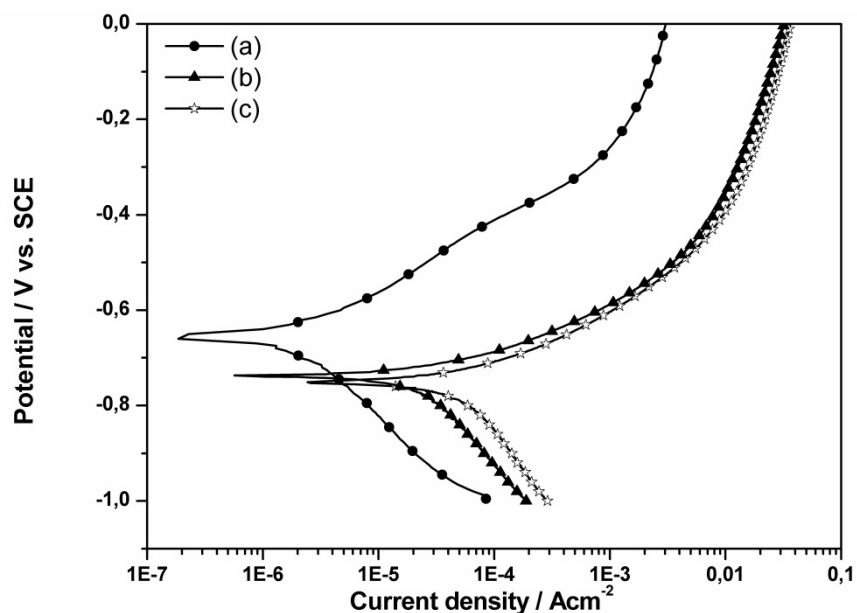


Fig.3. Voltametric curves obtained on carbon steel electrode in 0.01M NaCl with the surface: (a) uncovered; (b) covered by Mos-Na; (c) covered by Mag-Na

Fig. 4 and Fig. 5 illustrate the relation between the corrosiveness of a clay and its CEC. Each figure is related to Mos and Mag bentonites. Each voltammogram on a figure has been obtained with a bentonite treated by Na^+ , K^+ or Ca^{2+} . For each voltammogram the anodic charge density is calculated by curve integration. On the top of each figure we present this charge density, which corresponds to iron dissolution, versus the CEC of each bentonite. Top figures are uniformly scaled.

Even if the current density growth appears at the same potential for both bentonites, the curve slope depends on the nature of the bentonite and also on the applied chemical treatment. The influence of chemical treatments on CEC has been studied and attributed to the specific swelling produced by each cation [25, 26]. In the top figures it is interesting to observe the linear relationship between the anodic charge density and the CEC.

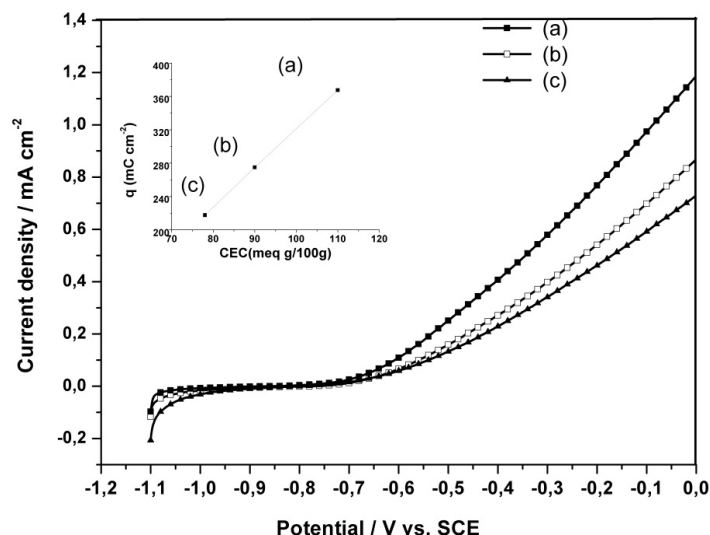


Fig.4. Voltamograms obtained in 0.01M NaCl solution with the working electrode covered by: (a) Mag-Na; (b) Mag-Ca; (c) Mag-K. The top figure shows the total anodic current obtained versus the CEC of the bentonite.

The anodic charge is in fact related to the amount of oxidised iron occurring at the steel surface. The linearity between the CEC and the charge density proves that when iron ion passes into the clay phase, it can't precipitate to form a protective passive film as it is known in aqueous media. With the presence of bentonite there is dissolution without precipitation. At anodic potentials the amount of dissolved iron ions depends on the ability of the bentonite to absorb cations which is indicated by its CEC.

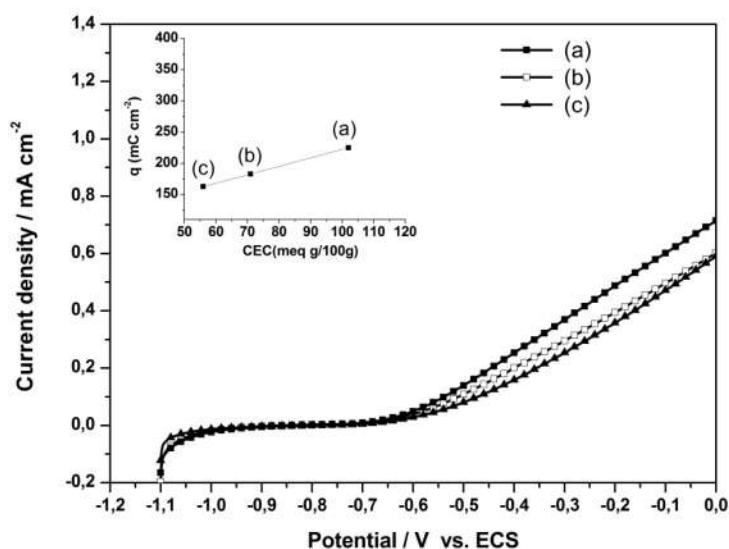


Fig 5. Voltamograms obtained in 0.01M NaCl solution with the working electrode covered by: (a) Mos-Na; (b) Mos-Ca; (c) Mos-K. The top figure shows the total anodic current obtained versus the CEC of the clay

Another interesting observation from the top figures is the difference of the curve slopes. An important slope indicates a more aggressive medium in the sense that high CEC causes more oxidation. The curve slope in Mag case is higher than in Mos case. The main difference between the two bentonites is their phase composition as reported on Table 1. Mag contains more montmorillonite than Mos, this increases its swelling properties and also its CEC which makes it more aggressive and increases the dissolution of iron.

Iron dissolution depends on CEC but also on other parameters as it is illustrated on Fig. 6. The figure gathers a set of voltammograms obtained in various situations. After each potential scan the steel surface is inspected and results are reported on Fig. 7. As it is expected and shown on Fig.7-a, a carbon steel surface exposed to a chloride containing solution exhibits pitting corrosion. Pits can appear on a carbon steel surface and their distribution is closely related to the steel phases as we shown in a previous work [25]. The apparent pitting potential corresponding to a sudden current density growth of Fig.6-a, depends on the presence of a passive film and can be shifted anodically or cathodically depending also on the pH.

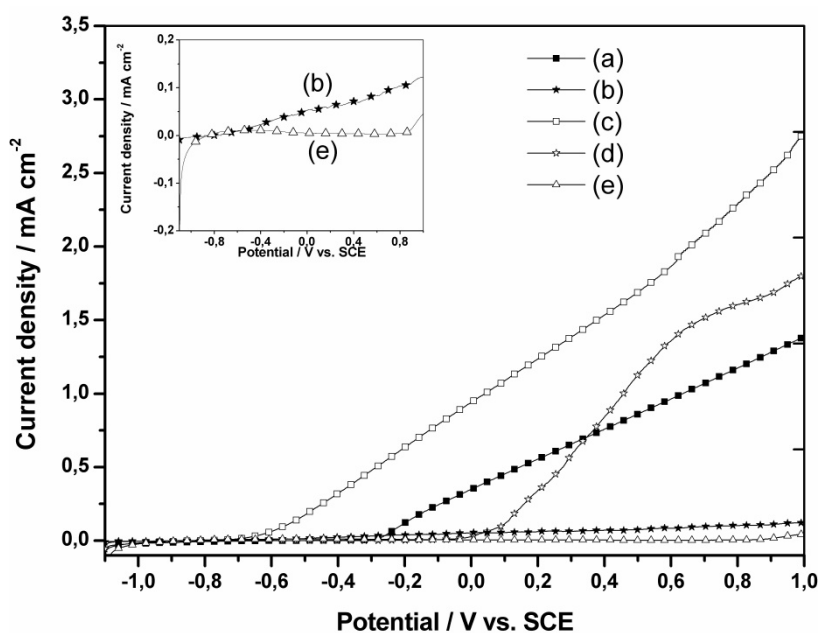


Fig.6. Voltammogram of a carbon steel in: (a): NaCl (0.01M); (b): Mag-Na/H₂O (deionised); (c): Mag-Na/NaCl (0.01M); (d): Mag-Na/ NaCl (0.01M) + Na₂WO₄ (0.01M); (e): Mag-Na (treated by Na₂WO₄)/ NaCl (0.01M)

Steel passivation doesn't occur in steel/clay systems since there is no precipitation process. This situation is illustrated by voltammogram Fig. 6-b and Fig. 7-b. The top voltammogram in Fig 6-b obtained after zooming shows a sudden current density growth starting at -700 mV

which corresponds in fact to the iron dissolution potential. So even if the aqueous solution doesn't contain aggressive agents the steel undergoes localised corrosion. Without pitting agents we can still observe a low but regular current density growth with the potential corresponding to continuous iron dissolution. This confirms the absence of passive films in steel/clay systems.

In addition to localised corrosion induced by the clay, inserting chloride to the solution causes the occurrence of pits as it is shown on Fig.7-c.

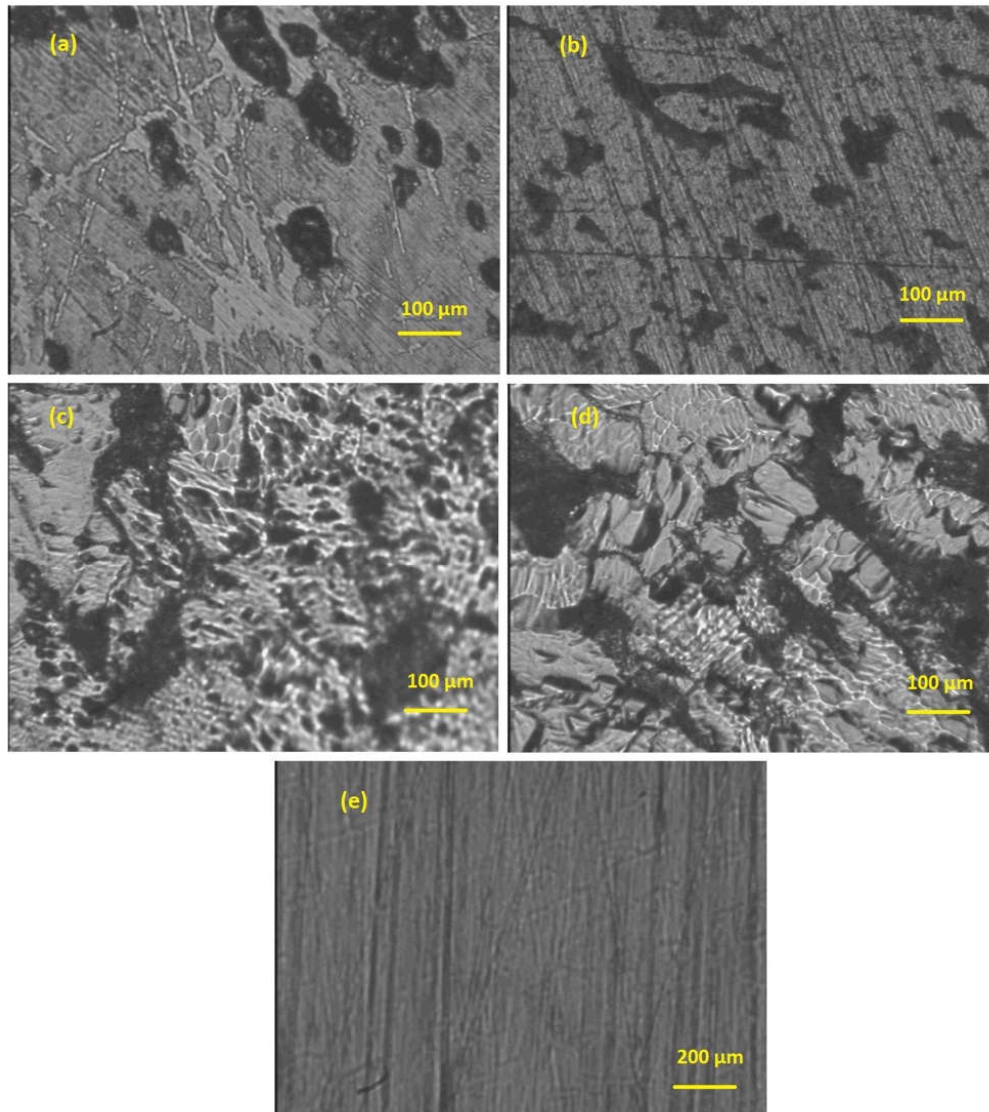


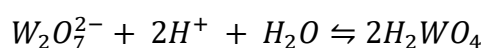
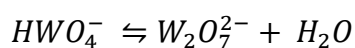
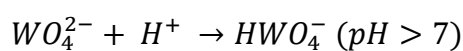
Fig.7. Surface observations after a voltammogram sweep in: (a): 0.01M NaCl; (b): deionised water and the surface covered by Mag-Na; (c): 0.01M NaCl and the surface covered by Mag-Na; (d): 0.01M NaCl + 0.01M Na₂WO₄ and the surface covered by Mag-Na; (e): 0.01M NaCl and surface covered by Mag-Na treated by tungstate

The voltammogram 6-c obtained in this situation shows a clear current density growth just after the iron dissolution potential. The presence of pits at the surface proves that chloride ions can cross through the clay and constitute a real threat to the steel integrity [12, 26].

In metal/aqueous solution systems corrosion and corrosion inhibition processes depend on both phases properties: pH, composition, phase proportions and so on. With such bi-phase systems, improving corrosion inhibition can be done by introducing inhibitors into one of the two phases: for example Ni, Cr, Mo in the steel or oxyanions in the solution. In steel/clay/aqueous solution corrosion and corrosion inhibition processes are even more complex [27]. But it remains possible to imagine that corrosion inhibition can also be made by a chemical treatment of the clay [28,29].

In this study, two cases are taken into consideration: clay previously enriched by inhibitors and inhibitors directly introduced into the aqueous solution. We used tungstate as corrosion inhibitor. The results are summarised on the voltammograms of Fig. 6-c, d and e, and the relative surface observations of Fig.7-c, d and e. The first case corresponds to the absence of tungstate and the presence of chloride in the solution. In the second case, tungstate is added to the solution. While in the last case, tungstate anions are added to the clay by a chemical treatment as explained before.

In presence of chloride and through the abrupt current density growth of Fig.6-c, it appears that pitting corrosion occurs just after the open circuit potential. The surface examination shows the presence of both localised corrosion and pits. Localised attacks are caused by the inhomogeneity of the clay but the pits are the result of the chloride presence. The addition of tungstate to the solution allows shifting anodically the current density (Fig.6-d). In this case the surface observation shows a substantial reduction of pits; however, localised attacks due to the clay remain. But when the tungstate is already present on the clay (e) no pitting occurs at any potential as it is confirmed by the zoom. Indeed, the very low current density at high potentials proves that no iron dissolution occurs at the steel/clay interface. This corrosion inhibition efficiency due to the tungstate presence on the clay is confirmed by the surface observation on Fig. 7-e where we notice that there is no corrosion at all, the acid medium of the pits favors the polymerisation of these oxyanion such as [30]:



The results prove that corrosion inhibition remains minor when tungstate comes from the solution. We can conceive that the presence of this anion on the solution reduces just the clay/solution interfacial concentration of chloride. But when tungstate is on the clay it reduces simultaneously its CEC and creates a strong barrier to chloride diffusion.

To complete the previous study, we performed a series of electrochemical impedance measurements in order to propose an electric equivalent circuit representing the various processes. Fig. 8 shows a voltammogram with four potentials at which impedance measurements have been performed.

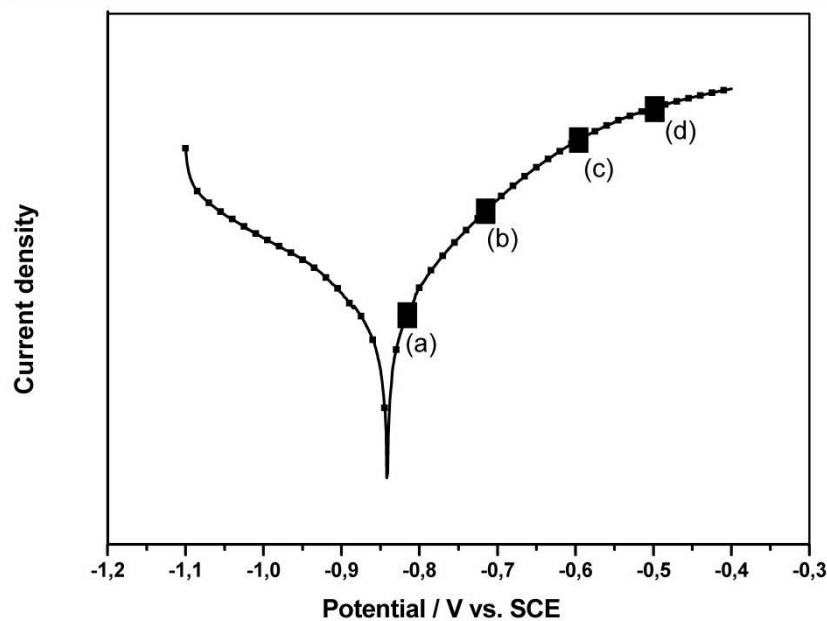


Fig.8. Voltammogram of carbon steel/Mag-Na/0.01M NaCl indicating four potentials at which EIS measurements have been made: a: -800; b:-700; c:-600; d:-500 mV/SCE

Impedance measurements start after 1 hour polarisation at a selected potential point. Fig. 9 and Fig. 10 are related respectively to Mag-Na and Mos-Na. On each figure four Nyquist diagrams are collected at each potential of the Fig. 8.

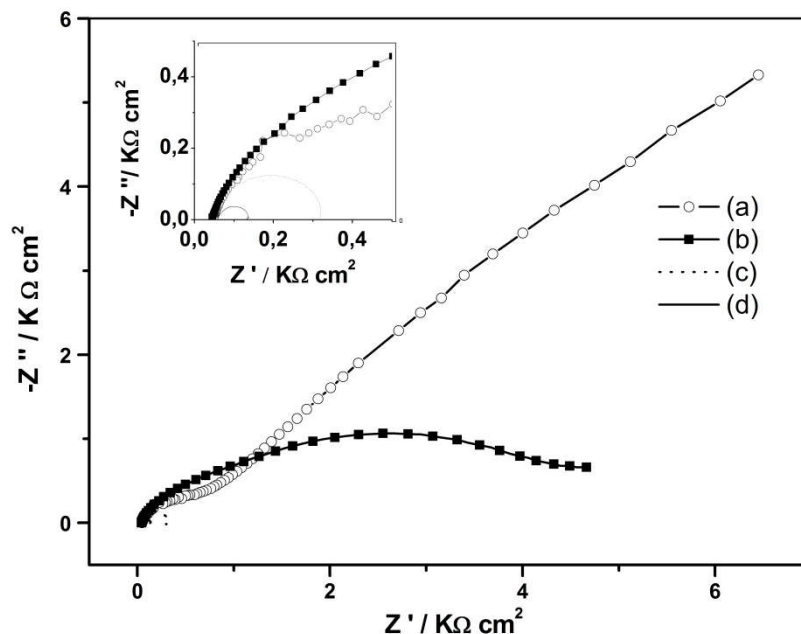


Fig.9. Nyquist plot for carbon steel/Mag-Na/0.01M NaCl after 1 hour polarisation at: a: -800; b:-700; c:-600; d:-500 mV/SCE

The shape of Nyquist curves at a given potential is roughly similar for both clays. For these three phases systems, it is possible to admit the presence of three semi circles as it is evident at -700 mV. By shifting the potential, the shapes and importance of these circles change.

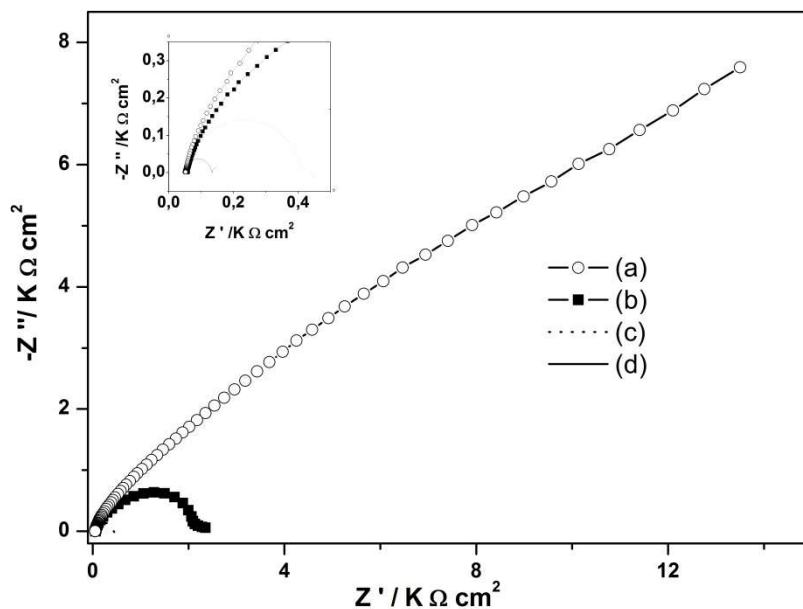


Fig.10. Nyquist plot for carbon steel/Mos-Na/0.01M NaCl after 1 hour polarisation at: a: -800; b:-700; c:-600; d:-500 mV/SCE

At a high potential the shape of the curves evolves from a semi-circle followed by a Warburg line to a simple semi-circle. These three phases' systems can be represented by equivalent electric circuits as shown on Fig. 11.

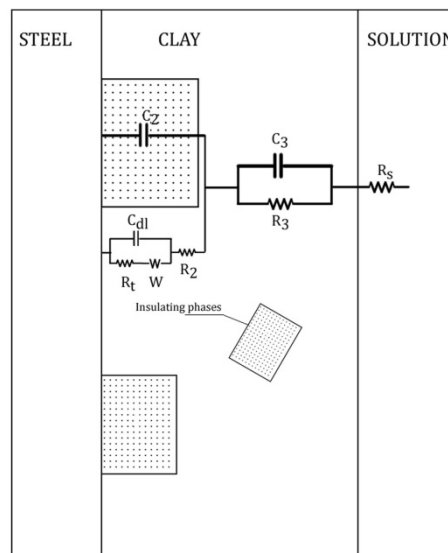


Fig.11. Electric equivalent circuit for the studied carbon steel/clay/solution

Faradic reactions occurring at the steel/clay interface are represented by R_t . C_d represents the double layer capacity. As the clay material encloses various phases, some of them are insulators and act as a barrier for chemical reactions at the steel/clay interface. We assimilate the system equivalent to that related to two superimposed porous layer studied by Bousselmi [31] in which a capacity C_2 represents charge distribution across this insulating phases and R_2 represents the discontinuity resistance of the region close to the interface. The volume of the clay can be represented by a parallel RC unit where R_3 and C_3 represent the resistance and the capacity of the charge distribution across the clay. R_s represents the solution resistance. In addition, a Warburg element (W) has been introduced and represents the diffusion processes. With this configuration a fitting has been made on experimental points obtained with Mag-Na at -700 mV/SCE. Experimental points and simulated curve are represented on Fig. 12 where we can see that the fitting is well done. The obtained values of the electrical components are grouped on Table 4.

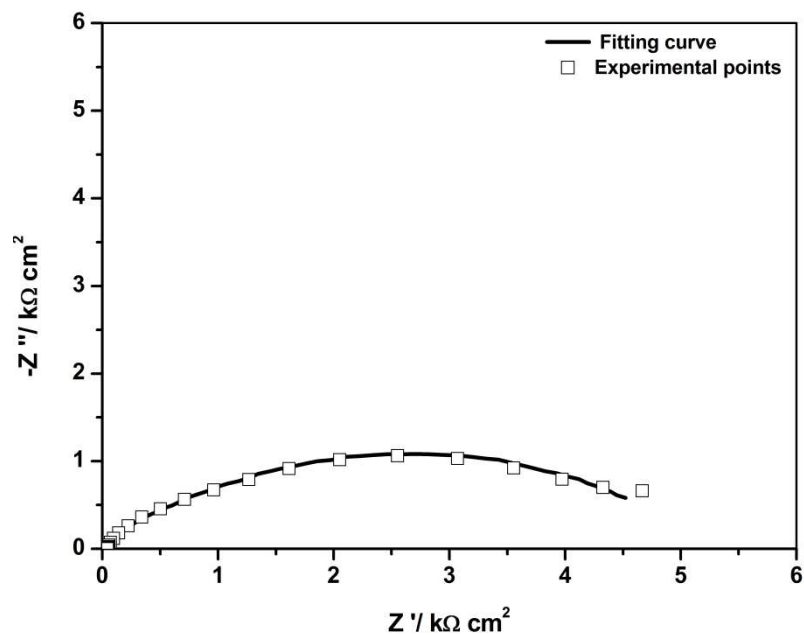


Fig.12. Experimental points and a fitting curve for carbon steel/Mag-Na/0.01M NaCl after 1 hour polarisation at -700 mV/SCE

Table 4. EIS Fitting results with Mag-Na at -700 mV/SCE

Potential [mV/ SCE]	EIS Fitting results with Mag-Na
-700	Rs= 65.31 Ohm
	C3= $2.16 \cdot 10^{-5}$ F
	R3= $1.64 \cdot 10^2$ Ohm
	C2= $1.14 \cdot 10^{-5}$ F
	R2= 40.75 Ohm
	Cdl= $5.95 \cdot 10^{-5}$ F
	Rt= $1.51 \cdot 10^{-3}$ Ohm
	W= $4.07 \cdot 10^{-5}$ S-sec ⁵

At -800 mV/SCE the potential is close to the OCP. Both materials show a straight line. At this potential the amount of oxidation and reduction products is not so important to sustain a high diffusion process. By increasing potential iron oxidation is favoured inducing a gradient of the products concentration across the clay. The clay becomes conducting and the three loops system can be reduced to a one loop system. In these conditions both clays present similar behaviour.

When clays are treated by tungstate we obtain the Nyquist curves of Fig. 13. The four curves have been obtained with both clays and at two different potentials. In all the cases we observe just a straight line which proves that processes taken place in clays treated by tungstate are limited by diffusion processes. This result is consistent with the curve of Fig. 6-e and the microscopic observation of Fig. 7-e. At this level of the observations we can state that tungstate affects essentially the diffusion processes but it remains possible that an eventual reaction leading to the formation of polyoxyanions at the steel/clay interface can take place.

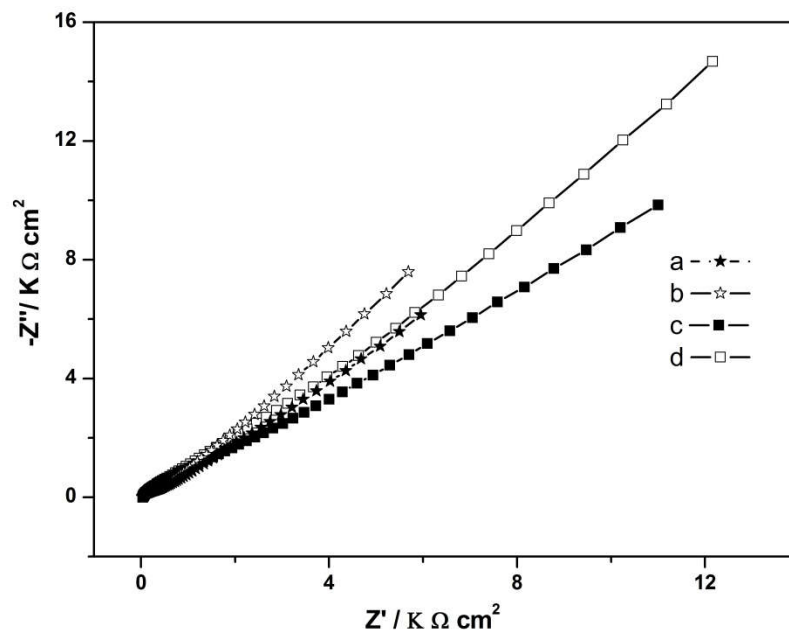


Fig.13. Nyquist plot for carbon steel/ tungstate treated bentonites (X) /0.01M NaCl after 1 hour polarisation at (Y) mV/SCE: (X,Y) = a: (Mag-Na, -800) ; b: (Mag-Na,-600) ; c: (Mos-Na,- 800) ; d: (Mos-Na,- 600)

In fact it has been proved that tungstate like molybdate have the characteristics to form various polyoxyanions at the points where localized corrosion appears [12].

4. CONCLUSION

The results of the work confirm that clay is intrinsically corrosive. This arises from the multiphase nature of the material and its cationic exchange capacity. Corrosion is even more serious if the system is subjected to an environment containing pitting agents such as chlorides. Yet the comparison between the two studied clays shows that Mag is slightly more corrosive than Mos. This difference must be solely related to the montmorillonite amount contained in the clay and implicitly to its CEC.

The observed corrosion inhibition efficiency of tungstate must also be related solely to CEC reduction. It is known that in a steel/aqueous system containing tungstate, local acidification around pits allows tungstate to form oxy-poly-anions which precipitate and stop pits evolution. But in a steel/clay/aqueous system such acidification is inconceivable as iron dissolution can't be followed by an hydroxylation.

To do this work we realized and validate an original corrosion study system adjusted to metal/clay/aqueous solution. Results are reproducible and quit acceptable. An adaptation of this system for measurements at high temperatures and pressures, which correspond to the storage conditions of radioactive waste, will provide more information and will allow to discern differences in the performances of clays.

5. NOMENCLATURE AND ABBREVIATION

Mag: Bentonite comes from the deposit of Hammam Boughrara in Maghnia Algeria.

Mos: Bentonite comes from the deposit of M'Zila in Mostaganem Algeria.

W %: Weight percentage.

CEC: Cationic Exchange Capacity.

EIS: Electrochemical Impedance Spectroscopy.

OCP: Open Circuit Potential.

SCE: Saturated Calomel Electrode.

Ecorr: Corrosion Potential.

Z: Electric Impedance.

6. REFERENCES

- [1] Lennemann W L, Parker H E, West P J. Management of radioactive wastes. *Annals of Nuclear Energy*, 1976, 3, (5-6), 285–295. doi:10.1016/0306-4549(76)90055-4
- [2] Gascoyne M, Gascoyne S S, Sargent F P. Geochemical influences on the design, construction and operation of a nuclear waste vault. *Applied Geochemistry*, 1995, 10, (6), 657–671. doi:10.1016/0883-2927(95)00034-8
- [3] Malone C R. Geologic and Hydrologic Issues Related to Siting a Repository for High-level Nuclear Waste at Yucca Mountain, Nevada, U.S.A. *Journal of Environmental Management*, 1990, 30, (4), 381-396. doi:10.1016/0301-4797(90)90030-Z

-
- [4] Kanwar R. Commissioning and operation of high level radioactive waste vitrification and storage facilities: the Indian experience. *Int. J. of Nuclear Energy Science and Technology*, 2005, 1, (2-3), 148-163. doi:10.1504/IJNEST.2005.007138
- [5] Dautray R, Friedel J, Bréchet Y. Nuclear energy in France today and tomorrow: IInd to IVth generations. *Comptes Rendus Physique*, 2012, 13, (5), 480-518. doi:10.1016/j.crhy.2012.02.001
- [6] Rempe N T. Permanent underground repositories for radioactive waste. *Progress in Nuclear Energy*, 2007, 49, (5), 365-374. doi:10.1016/j.pnucene.2007.04.002
- [7] Marty N C M, Fritz B, Clément A, Michau N. Modelling the long term alteration of the engineered bentonite barrier in an underground radioactive waste repository. *Applied Clay Science*, 2010, 47, (1-2), 82-90. doi:10.1016/j.clay.2008.10.002
- [8] Eisenberg N A, Sagar B. Importance measures for nuclear waste repositories. *Reliability Engineering and System Safety*, 2000, 70, (3), 217-239, doi:10.1016/S0951-8320(00)00050-8
- [9] Féron D, Crusset D, Gras J. Corrosion issues in nuclear waste disposal. *Journal of Nuclear Materials*, 2008, 379, (1-3), 16-23. doi:10.1016/j.jnucmat.2008.06.023
- [10] Martin F A, Bataillon C, Schlegel M L. Corrosion of iron and low alloyed steel within a water saturated brick of clay under anaerobic deep geological disposal conditions: An integrated experiment. *Journal of Nuclear Materials*, 2008, 379, (1-3), 80-90. doi:10.1016/j.jnucmat.2008.06.021
- [11] Ishidera T, Ueno K, Kurosawa S, Suyama T. Investigation of montmorillonite alteration and form of iron corrosion products in compacted bentonite in contact with carbon steel for ten years. *Phys. Chem. Earth*, 2008, 33, (1), 269-275. doi:10.1016/j.pce.2008.10.062
- [12] Jeannin M, Calonnec D, Sabot R, Refait P. Role of a clay sediment deposit on the corrosion of carbon steel in 0.5 mol L⁻¹ NaCl solutions. *Corrosion Science*, 2010, 52, (6), 2026-2034. doi:10.1016/j.corsci.2010.02.033
- [13] Bildstein O, Trotignon L, Perronnet M, Julien M. Modelling iron–clay interactions in deep geological disposal conditions. *Phys. Chem. Earth*, 2006, 31, (10-14), 618-625. doi:10.1016/j.pce.2006.04.014
- [14] Carlson L, Karnland O, Oversby V, Rance A P, Smart N R, Snellman M, Vähänen M, Werme L O. Experimental studies of the interactions between anaerobically corroding

- iron and bentonite, *Phys. Chem. Earth*, 2007, 32, (1-7), 334-345. doi:10.1016/j.pce.2005.12.009
- [15] Jabeera B, Shibli S M A, Anirudhan T S. Synergistic inhibitive effect of tartarate and tungstate in preventing steel corrosion in aqueous media. *Applied Surface Science*, 2006, 252, (10), 3520-3524. doi:10.1016/j.apsusc.2005.05.029
- [16] Boucherit M N, Amzert S, Arbaoui F, Hanini S, Hammache A. Pitting corrosion in presence of inhibitors and oxidants. *Anti-Corrosion Methods and Materials*, 2008, 55, (3), 115-120. doi:10.1108/00035590810870419
- [17] Arbaoui F, Boucherit M N. Comparison of two Algerian bentonites: physico-chemical and retention capacity study. *Applied Clay Science*, 2014, 91-92, 6-11. doi:10.1016/j.clay.2014.02.001
- [18] Ortiz M R, Rodriguez M A, Carranza R M, Rebak R B. Oxyanions as inhibitors of chloride-induced crevice corrosion of Alloy 22. *Corrosion Science*, 2013, 68, 72-83. doi:10.1016/j.corsci.2012.10.037
- [19] Boukhari Y, Boucherit M N, Zaabat M, Amzert S, Brahimi K. artificial intelligence to predict inhibition performance of pitting corrosion. *Journal of Fundamental and Applied Sciences*, 2017, 9(1), 308-322. doi: 10.4314/jfas.v9i1.19
- [20] Alghem L, Ramdhane M, Khaled S. The development and application of k(0)-standardization method of neutron activation analysis at Es-Salam research reactor. *Nuclear instruments & methods in physics research*, 2006, 556, (1), 386-390. doi:10.1016/j.nima.2005.10.017
- [21] Yukselen Y, Kaya A. Suitability of the methylene blue test for surface area, cation exchange capacity and swell potential determination of clayey soils. *Engineering Geology*, 2008, 102, (1-2), 38-45. doi:10.1016/j.enggeo.2008.07.002
- [22] Boucherit M N, Tebib D. A study of carbon steels in basic pitting environments. *Anti-Corrosion Methods and Materials*, 2005, 52(6), 365-370, doi:10.1108/00035590510624703
- [23] Li Y, Wu B, Zeng X, Liu Y, Ni Y, Zhou G, Ge H. The voltammetry–photocurrent response study of passivation of carbon steel in slightly alkaline solutions containing the corrosion inhibitor phosphor-polymaleic acid–ZnSO₄. *Thin Solid Films*, 2002, 405, (1-2), 153-161. doi:10.1016/S0040-6090(01)01730-8
- [24] Johnson L, King F. The effect of the evolution of environmental conditions on the corrosion evolutionary path in a repository for spent fuel and high-level waste in

- Opalinus Clay. *Journal of Nuclear Materials*, 2008, 379, (1-3), 9-15. doi:10.1016/j.jnucmat.2008.06.003
- [25] Teppen B J, Miller D M. Hydration energy determines isovalent cation exchange selectivity by clay minerals. *Soil Science Society of America Journal*, 2006, 70, (1), 31-40. doi:10.2136/sssaj2004.0212
- [26] Ferrage E, Lanson B, Sakharov B A, Drits V A. Investigation of smectite hydration properties by modeling experimental X-ray diffraction patterns: Part I Montmorillonite hydration properties. *American Mineralogist*, 2005, 90, (8-9), 1358-1374. doi:10.2138/am.2005.1776
- [27] Honda A, Teshima T, Tsurudome K, Ishikaw H, Yusa Y, Sasaki N. Effect of compacted bentonite on the corrosion behaviour of carbon steel as geological isolation over pack material. *Materials Research Society Symposium Proceedings (Materials Research Society, Pittsburgh, PA)*, 1991, 212, 287-294. doi:10.1557/PROC-212-287.
- [28] Zaiz T., Lanez T. Application of some ferrocene derivatives in the field of corrosion inhibition. *Journal of Chemical and Pharmaceutical Research*, 2012, 4(5):2678-2680.
- [29] Lanez T. et al. Electrochemical study and computational details of copper corrosion inhibition by 1h-benzotriazole in 3 % wt. NaCl medium, *Mor. J. Chem.* 2015, 3(2) 809-823.
- [30] Guo Y., Li D., Hu C., Wang Y., Wang E., Zhou Y., Feng S. Photocatalytic degradation of aqueous organochlorine pesticide on the layered double hydroxide pillared by Paratungstate A ion, $Mg_{12}Al_6(OH)_{36}(W_7O_{24})_4H_2O$. *Applied Catalysis B: Environmental*, 2001, 30 (4) 337–349. doi:10.1016/S0926-3373(00)00246-0
- [31] Bousselmi L, Fiaud C, Tribollet B, Triki E. Impedance Spectroscopic Study of a Steel electrode in Condition of Scaling and Corrosion: Interphase Model. *Electrochimica Acta*, 1999, 44, (24), 4357-4363. doi:10.1016/S0013-4686(99)00151-6.

How to cite this article:

Arbaoui F, Amzert SA, Boucherit MN. Corrosion of a carbon steel covered by treated bentonites in aqueous solution. *J. Fundam. Appl. Sci.*, 2017, 9(3), 1300-1319.